*Manuscript
Click here to view linked References

Metal-silicate silicon isotopic fractionation and the composition of the bulk Earth

Frédéric Moynier[1], Zhengbin Deng[1], Ariane Lanteri[1], Rayssa Martins[1], Marc Chaussidon[1], Paul Savage[2], Julien Siebert[1,3]

[1]Institut de Physique du Globe de Paris, Université de Paris, CNRS, 1 rue Jussieu, Paris 75005, France

[2]School of Earth and Environmental Sciences, University of St Andrews, Irvine Building, St Andrews, KY16 9AL, United Kingdom

[3]Institut Universitaire de France, 103 boulevard Saint-Michel, Paris 75005, France

moynier@ipgp.fr

Abstract:

The difference in the Si isotopic composition between the Earth and primitive meteorites had been used to constrain the amount of Si in the Earth's core. However, there is presently a debate on the magnitude of the isotopic fractionation between metal and silicates as function of temperature based on experimental data. Here, we use a natural sample, an enstatite meteorite, Itqyi, as a natural experiment to determine an independent Si isotopic fractionation factor between metal and silicate. We determined the temperature of equilibrium between metal and silicate as well as the Si isotopic composition between the phases. We find that the dependence of Si isotopes with

temperature to be :

$$\Delta^{30}Si_{silicate-metal} = \frac{7.6\ (\pm 0.7) \times 10^6 (1SD)}{T^2}$$

Using this dependence of the δ^{30}Si with temperature we estimate the bulk Earth δ^{30}Si as a function of Si content of the core for different plausible conditions. Even when using the most extreme parameters, we show that the bulk Earth must be isotopically heavier than any chondrites groups. We therefore confirm that core formation alone cannot account for the isotopic difference between the Earth and primitive meteorites. We show that there is no correlation between δ^{30}Si and the Mg/Si ratio suggesting that forsterite fractionation in the solar nebula may have had only a limited effect, if any. Our new results therefore confirm that volatility should have had a fundamental effect in shaping terrestrial planets chemical composition.

1. Introduction

In order to explain the deficit in density of the Earth's outer core it must contain ~10% of elements lighter than Fe (Birch, 1964). While, the nature of these lighter elements is still debated, high-pressure high-temperature experiments show that it is most likely composed of O, Si and S (e.g. Badro et al., 2015; Righter and Drake, 2003; Siebert et al., 2013).

Because they are potentially fractionated between metal and silicate, stable isotopes have been employed as independent tracers of core formation and composition (e.g. Bonnand and Halliday, 2018; Creech et al., 2017; Fitoussi et al., 2009; Georg et al., 2007; Hin et al., 2013; Hopp et al., 2018; Mahan et al., 2018; Roskosz et al., 2006; Savage et al., 2015; Shahar et al., 2017; Shahar et al., 2009; Ziegler et al. 2010). In particular it has been demonstrated that the $^{30}Si/^{28}Si$ of the silicate Earth is ~0.15 ‰ (per mil) heavier than those undifferentiated meteorites argued to represent the composition of the bulk Earth (e.g. Armytage et al., 2011; Fitoussi et al., 2009; Georg et al., 2007; Zambardi et al., 2013; Poitrasson 2017). This excess in the heavier isotopes in the silicate Earth is supposedly compensated by an isotopically light core (e.g. Georg et al., 2007) and using estimates of the equilibrium isotopic fractionation between metal and silicate it is possible to calculate the amount of Si that must be stored in the Earth core to explain the observed isotopic difference, assuming no other source of isotopic fractionation (e.g. Hin et al. 2014; Savage et al., 2014; Shahar et al., 2009; Ziegler et al. 2010). However, there is debate over the magnitude of Si isotope fractionation between metal and silicate at equilibrium: the two experimental approaches, based on high-pressure and high-temperature experiments using a piston-cylinder press return

57 different results, with Hin et al. (2014) calculating a smaller degree of isotopic
58 fractionation than Shahar et al. (2009) at the temperatures relevant to core formation.
59 The degree of this difference is significant, as using the Hin et al. (2014) isotopic
60 fractionation factor would either require an unrealistic amount of Si present in the core
61 (whatever chondrites type used as starting composition) to explain the silicate Earth
62 composition, if core formation was the only process which has affected the Si isotope
63 composition of the BSE since Earth's formation.

64 An alternative and complementary approach would be to use natural samples that
65 contain equilibrated metal and silicate with measurable amounts of Si partitioned into
66 the metal. However, samples fitting this requirement (metal and silicate that
67 equilibrated at low fO_2 conditions) are rare and so far only two samples have been
68 studied (Ziegler et al., 2010). Using two enstatite achondrites, which equilibrated at
69 similar temperatures (1200 K and 1130K), Ziegler et al. (2010) measured the difference
70 in Si isotopic composition between metal and silicate. Their results are in agreement
71 with the experimental curve determined by Shahar et al. (2009), and fall off that
72 determined by Hin et al. (2014), although, since both meteorites analyzed here, Mount
73 Egerton and Norton County, equilibrated under similar temperature, it only provides
74 one data point to the calibration curve.

75 The hypothesis behind the above approaches is that the Si isotopic difference
76 between the BSE and chondrites is uniquely controlled by core formation. The fact that
77 an unrealistic amount of Si may need to be stored in the Earth's core (e.g. Fitoussi and
78 Bourdon, 2012; Hin et al., 2014) together with the later discovery of heavy Si isotopic

composition in angrite meteorites representing the silicate fraction of a small oxidized (with *a priori* no Si in its core) de-volatized differentiated parent body suggest that volatility may exert a strong control on the Si isotopic composition of a planet, which have greatly changed our vision on how planet acquired their present chemical composition (e.g. Fitoussi et al., 2009; Hin et al., 2017; Pringle et al., 2014; Sikdar and Rai, 2020; Zambardi et al., 2013; Young et al., 2019). Based on a correlation between δ^{30}Si and Mg/Si, Dauphas et al. (2015) proposed an alternative scenario in which the enrichment in the heavy Si isotope represent gas-forsterite isotopic fractionation in the solar nebula. The Earth would be relatively depleted in refractory phases (forsterite), decreasing its Mg/Si ratio and increasing its δ^{30}Si. However, this approach needs also an estimate of δ^{30}Si of the bulk Earth and therefore relies on the Si isotopic fractionation during core formation.

Given the important implications cited above, it is therefore primordial to better constrain the exact Si metal-silicate isotopic fractionation factor, to establish the maximum effect of core formation on the Si isotopic composition of the Earth's mantle, in order to estimate the composition of the present bulk Earth. Here, we determine the Si isotopic fractionation between metal and silicate using a recently discovered meteorite, Itqyi. Itqyi is metal-rich and coarse-grained, regarded as an enstatite achondrite (e.g. Patzer et al., 2001; Patzer et al., 2002) which, similar to the samples utilized in Ziegler et al. (2010), equilibrated under very reduced conditions and partitioned several percent of Si into its metal phase. Since there have been very limited studies on Itqyi, we first demonstrate that metal and silicate phases are at equilibrium,

and determine the fO_2 and temperature of equilibrium based on elemental partitioning experiments. Finally, we present the Si isotopic composition of the metal and silicate phases. We will show that the temperature of metal/silicate equilibrium is different from the two meteorites used in Ziegler et al. (2010), which will allow us to provide a new independent isotopic fractionation factor at a different temperature, to test the previous estimates of the meta/silicate isotopic fractionation, estimate the maximum effect of core formation on the Si isotopic composition of the mantle, and propose a Si isotopic composition for the bulk Earth including different scenarios of core formation.

2. Samples and Methods

2.1 Samples

Itqyi is a coarse-grained enstatite achondrite mostly composed of enstatite (75%) and kamacite (25%), plus traces of sulfides (Patzer et al., 2001). We obtained several grams of the samples from Luc Labenne, the discoverer of Itqyi in the Western Sahara Desert in 2000. This meteorite has an igneous texture with metal percolation features between enstatite grains, triple junctions between enstatite grains and homogeneous composition of enstatite and metal grains suggesting partial melting and re-equilibration of the meteorite (Patzer et al., 2001). In order to estimate the elemental distribution in the metal and silicate grains we have cut and polished a ~1cm section of the sample (see Figure 1), mapped the sample with a field emission gun scanning electron microscope (FEG-SEM) and determined chemical profiles and phase

compositions with an electron probe microanalyzer (EPMA). We then selected and mechanically separated 6 silicate grains and 4 metal grains for Si isotopic analysis.

A sample of BHVO-2 (Hawaiian basalt, USGS standard) was analyzed following the same analytical methods for its Si isotopic composition, to evaluate the quality of the Si isotopic measurements.

2.2.EPMA

Metal and silicate phases of the samples were analyzed using a Cameca SX-five electron microprobe. Operating conditions were 15 kV accelerating voltage, 10 nA beam current and counting times of 10-20 seconds on peak and background for major and minor elements in silicate (Si, Mg, Fe, Al, Ca, Na, Ti and K). For trace elements (P, Co, Ni, Cr, V) in both metal and silicate, analyses were collected with 15 kV accelerating voltage, 100 nA beam current and counting times up to 50-100 seconds on peak and background. Diopside glass (Si), wollastonite (Ca), orthoclase (K), anorthite (Al), albite (Na), rutile (Ti) and pure oxides (Fe_2O_3, MgO, SiO_2, CaO and Al_2O_3) were used as standards for the major and minor elements. Pure metals were used as standards for the metal and trace elements except apatite for P and pyrite for S. To avoid secondary fluorescence contamination, silicate analyses were taken few tens of microns away from the metallic phases. Electron probe analyses of both metal and silicate phases are reported in Table 1.

2.3 Isotopic measurements

A thick section of Itqyi meteorite was crushed roughly using an agate mortar, and the enstatite and metal fragments were handpicked under a microscope. The selected

144 enstatite grains were fused in eight aliquots (2-3 mg for each aliquot) using NaOH as a
145 flux, at 720 °C in Ag crucibles (99.99% pure Ag at a trace metals basis). The fusion
146 cakes were placed in 30 mL Savillex beakers filled with 5-10 mL MQ-e H_2O (18.2 MΩ
147 cm^{-1}), and the beakers were then placed in an ultrasonic bath for 15 minutes. The
148 samples were then transferred with pipette into pre-cleaned 50 mL tubes by rinsing the
149 sample-bearing Ag crucibles three to four times with MQ-e H_2O. To avoid
150 over-acidification of the solutions, only 0.10-0.30 mL 16 M HNO_3 acid was added to
151 acidify the sample solutions till the sample solutions became clear so we reached a pH
152 of ~1. The metal fragments were dissolved in 8 M HNO_3 acid, and NaOH was added to
153 neutralize the solutions. Over these dissolution procedures, the NO_3^-/Si ratios in the
154 dissolved solutions were monitored, based on an existing observation that the Si
155 contents in enstatite and metal fractions of the Itqyi meteorite were 28 wt.% and 3 wt.%
156 respectively. Solution aliquots containing 20 μg Si from the Itqyi meteorite, BHVO-2
157 and NIST RM 8456 (historically, and from hereon called NBS28) were processed
158 through pre-cleaned BioRad Poly-Prep chromatography columns containing 1.8 mL
159 AG50X-12 (200-400 mesh) cation exchange resin to purify Si from matrix elements
160 (Georg et al., 2006). At low to neutral pH, Si is present as either neutral or anionic
161 species. Therefore, Si is eluted by MQ-e H_2O rinsing with other anions like NO_3^-, while
162 cations were kept on the columns by the AG50X-12 resin (Fujii et al., 2015). The full
163 blank for the procedure is 20 ng.

164 The Si concentration of the purified samples was set to be 2 ppm in 0.2 N HNO_3,
165 and were measured for Si isotopic composition on a Neptune plus multi-collector

inductively-coupled-plasma mass spectrometer (MC-ICP-MS) at the Institut de Physique du Globe de Paris (IPGP). Samples were analysed under "wet plasma" conditions via a quartz-made spray chamber. Isobaric interferences (in particular from $^{14}N^{16}O^{+}$ on $^{30}Si^{+}$) were avoided by measuring on the low mass peak shoulder under medium mass resolution mode ($M/\Delta M \approx 5000$). Under medium resolution mode, the typical sensitivity for a 2 ppm Si solution with an uptake rate of 100 μL/min is 10-12 V on $^{28}Si^{+}$, and the blank over the whole analytical session is 5-10 mV on $^{28}Si^{+}$. A sample-standard bracketing protocol was used in this study, i.e. measuring NBS28 standard once after each analysis on unknown samples. Each analysis contains 25 cycles with an integration time of 4 s for each cycle, and each sample was measured four or more times. The Si isotopic results of the studied samples are reported in per mil (‰) delta notation using both $^{30}Si/^{28}Si$ and $^{29}Si/^{28}Si$ ratios of the samples relative to those of the NBS28 quartz standard, i.e. $\delta^{30}Si$ and $\delta^{29}Si$, respectively (Table 2).

While the used AG50X-12 columns cannot remove NO_3^- from Si, it has been observed in this study that a mismatch of NO_3^- between sample and bracketing NBS-28 standard can lead to an artificial shift of sub per mil level on the measured Si isotopic ratio. For instance, a purified NBS28 aliquot with 0.44 M NO_3^- provides a $\Delta^{30}Si$ value of -0.46 ± 0.03 (2SE, n = 4) relative to another purified NBS28 aliquot with 0.2 M NO_3^- (Table 2). As such, aliquots of the fusion solution of NBS28 were doped properly with HNO_3 before being loaded on the AG50X-12 columns to reach similar NO_3^-/Si ratios as the processed aliquots of enstatite and metal samples. In detail, this match of NO_3^- (0.44 M) between BHVO-2 and NBS-28 successfully returned to a $\delta^{30}Si$ value of

188 −0.25 ± 0.05 (2SE, n = 4), which is identical to the recommended value (−0.28 ± 0.03;
189 Savage et al., 2014). Measurements on the NBS28 aliquots with 0.6 mg and 2.0 mg
190 dissolution masses provides δ^{30}Si value of +0.02 ± 0.03 (2SE, n = 4) and +0.03 ± 0.03
191 (2SE, n = 4), respectively, implying that the Si isotope protocol in this study is
192 applicable to the samples of small masses.
193
194 **3. Results**
195 The SEM (Figure 1) and EPMA analyzes of Si and Fe content (Table 1) confirm the
196 igneous coarse texture and the absence or very limited elemental zoning of the
197 meteorite (Patzer et al. 2001). The 120 degrees angles between grains are characteristic
198 of partial melting and the percolation of metal between the enstatite grains (Figure 1)
199 confirms the partial melting of the meteorite parent body (Patzer et al., 2001).
200 The EPMA Fe and Si abundance profile (Figure S1), show very homogeneous
201 distributions within the grains. The exception being at the grain boundary, within
202 50-100μm (Figure S1) which may reflect contamination of the signal by secondary
203 X-ray fluorescence from the adjacent metal or silicate grain. The rest of the grains are
204 fairly homogeneous and we use the average composition of the EMPA profile as the
205 average composition of the grain. For example, the metal grain #1 (M1) is in contact
206 with enstatite grain #1 (E1) and enstatite grain #2 (E2). When the first 100μm of the
207 silicate grain is excluded we obtain an average composition for Si (27.73 ± 0.16
208 weight%, 27.88 ± 0.24 weight%) and Fe (0.07 ± 0.02 weight%, 0.05 ± 0.03 weight%)
209 content in E1 and E2 similar within 1SD.

The isotopic composition of BHVO-2 and of the metal and silicate grains of Itqyi are reported in the Table 2. All the data are reported using the δ^{x}Si notation, which is the per mil deviation of the $^{x}Si/^{28}Si$ ration from the NIST NBS28 standard (x = 29 or 30). All the data reported here are mass-dependent, and only δ^{30}Si will discussed below. When not specified, the error discussed below for the δ^{30}Si are the 2 standard deviation.

The δ^{30}Si of two independently processed BHVO-2 (-0.26 ± 0.02 and -0.25 ± 0.05) are in excellent agreement with previous literature data (e.g. Abraham et al., 2008; Fitoussi et al., 2009; Pringle et al., 2013; Savage et al., 2010) and the δ^{30}Si of metal and silicate of Itqyi is similar to what had been previously measured for other aubrite-like rocks (Ziegler et al. 2010).

The δ^{30}Si of the 8 silicate grains are very homogeneous with an average of -0.57 ± 0.05 (2SE, n = 8). The δ^{30}Si of the 5 metal grains are slightly more variable with an average of -3.44 ± 0.19 (2SE, n = 5). When taken together and the error is propagated the difference between the δ^{30}Si of the silicate and metal phase $\Delta^{30}Si_{silicate\text{-}metal}$=2.87 ± 0.20 (2SE).

4. Discussion

We first estimate the fO_2 and T of equilibrium for the metal and silicate phases. The fO_2 can be determined by basing it on the oxidation equation of Fe:

$$Fe + \frac{1}{2}O_2 = FeO, \quad \text{Eq. 1}$$

and defining the fO2 relative to its deviation from the Iron-Wustite buffer (ΔIW), defined as:

$$\Delta IW = 2log\left(\frac{a_{FeO}^{silicate}}{a_{Fe}^{metal}}\right) = 2log\left(\frac{x_{FeO}^{silicate}}{x_{Fe}^{metal}}\right) + 2log\left(\frac{\gamma_{FeO}^{silicate}}{\gamma_{Fe}^{metal}}\right). \quad \text{Eq. 2}$$

In equation 2, $a_{FeO}^{silicate}$ and a_{Fe}^{metal} are the activities of FeO in the silicate and Fe in the metal respectively, $x_{FeO}^{silicate}$ and x_{Fe}^{metal} are the molar fractions of FeO in the silicate and Fe in the metal respectively, and $\gamma_{FeO}^{silicate}$ and γ_{Fe}^{metal} are the activity coefficients of FeO in the silicate and Fe in the metal. If we assume ideal behavior, the activity coefficients are equal to unity, and the equation becomes:

$$\Delta IW = 2log\left(\frac{x_{FeO}^{silicate}}{x_{Fe}^{metal}}\right). \quad \text{Eq. 3}$$

By using the average composition of the silicate and metals determined by EPMA (Figure S1) and by propagating the errors we obtain ΔIW = -6.6 ± 0.8. This value is consistent with equilibrium under very reduced conditions, similar to those estimated for enstatite chondrites (Berthet et al., 2009).

The temperature of equilibrium can be estimated by comparing the distribution coefficients of Si and Cr to experimental results. The distribution of Si and Cr between metal and silicate is controlled by the following redox exchange reactions with Fe:

$$2Fe^{metal} + SiO_2^{silicate} = 2FeO^{silicate} + Si^{metal} \text{Eq. 4).}$$

$$Fe^{metal} + CrO^{silicate} = FeO^{silicate} + Cr^{metal} \text{ (Eq. 5).}$$

The equilibrium constant of these reactions can be expanded in terms of mole fractions, activity coefficients and thermodynamic constants following:

$$logK\,(Si) = log\left(\frac{{x_{Si}^{metal}}/{x_{SiO2}^{silicate}}}{\left({x_{Fe}^{metal}}/{x_{FeO}^{silicate}}\right)^2}\right) + log\left(\frac{{\gamma_{Si}^{metal}}/{\gamma_{SiO2}^{silicate}}}{\left({\gamma_{Fe}^{metal}}/{\gamma_{FeO}^{silicate}}\right)^2}\right) = a + \frac{b}{T} + c.\frac{P}{T}, \quad \text{Eq. 6}$$

$$logK\ (Cr) = log\left(\frac{{x_{Cr}^{metal}}/{x_{CrO}^{silicate}}}{\left({x_{Fe}^{metal}}/{x_{FeO}^{silicate}}\right)}\right) + log\left(\frac{{\gamma_{Cr}^{metal}}/{\gamma_{CrO}^{silicate}}}{\left({\gamma_{Fe}^{metal}}/{\gamma_{FeO}^{silicate}}\right)}\right) = a + \frac{b}{T} + c.\frac{P}{T} \quad \text{Eq. 7}$$

where a, b, c are regression constants standing for the entropy, enthalpy, and volume change of reactions (4) and (5) divided by the gas constant (i.e. ΔrS°/R, ΔrH°/R, and ΔrV°/R respectively), T the temperature in K and P the pressure in GPa. The metal silicate partitioning of Si and Cr have been extensively studied in high pressure and high temperature experiments (e.g. Corgne et al., 2008; Fischer et al., 2015; Siebert et al., 2013; Siebert et al., 2011; Wade and Wood, 2005)) leading to different expressions for the parameterization of the equilibrium constants of Eq. 6 and Eq. 7. The effect of pressure on the partitioning of these two elements is negligible and these datasets can be suitable for modeling the conditions of equilibration of Itqyi. Using the regression constants and activity models for Si and Fe in the metal from Corgne et al. (2008), Siebert et al. (2013) and Fischer et al. (2015), we calculate that the measured concentrations of Si and Fe in the metal and silicate phases of Itqyi equilibrated at an approximate temperature of 1530 K ± 110 K.

Note here that each of the above studies treat differently the ratios of activity coefficients of oxides in the silicate $\left({\gamma_{FeO}^{silicate^2}}/{\gamma_{FeO}^{silicate}}\right)$ (which represents the effect of silicate composition on the partitioning of Si). This parameter was either considered constant as in Siebert et al. (2013) and Fischer et al. (2015) or was modeled

by using the non-bridging oxygen over tetrahedra structural parameter as a proxy as in Corgne et al. (2008). In an effort to best constrain the temperature of equilibrium, we consider that the particular experiments conducted in Corgne et al. (2008) represent a good approximation of the conditions of P-T-fO_2, and both metal and silicate compositions present during the equilibration of the Itqyi achondrite. Using regression parameters from Corgne et al. (2008) only lead to the highest T estimate for Itqyi metal-silicate equilibration of 1650 K ± 90 K.

The same above approach is followed using the Cr and Fe concentrations in metal and silicate of Itqyi from Eq. (7). The regression constants and activity models of Eq. (7) for Cr in metal are taken after Siebert et al. (2013) which represents an exhaustive compilation of the existing dataset for Cr partitioning. Using Cr, a T of 1400 ± 240 K is derived for the metal-silicate equilibration of Itqyi in good agreement with the T estimated using Si partitioning data. In the following we consider the estimate based on Si partitioning data rather than Cr as it is more precise.

Here we show that enstatite and metal equilibrated in Itqyi under fO_2 of ΔIW-6.6 and at a temperature of 1530 K ± 110 K. Note that using the approach developed in Wasson (1994) leads to a similar T of equilibration of about 1500 K. This temperature is ~300-400 K higher than estimated for Mount Egerton and Norton County by Ziegler et al. (2010) and by combining both studies we can add a second data point with which to better constrain the variation of $\Delta^{30}Si_{silicate\text{-}metal}$ as a function of temperature.

Combining the temperature estimated above (T=1530 ± 110 K) with $\Delta^{30}Si_{silicate\text{-}metal}$= 2.98 ± 0.18 (2SD) we can calculate the temperature dependence for

isotopic fractionation by simply fitting a $1/T^2$ curve through our data point (we report the error on the fit as 1SD error to be consistent with previous work Ziegler et al., 2010, see Figure 2). The error includes uncertainties on the isotopic fractionation factor and on the temperature of equilibrium. This returns a parametrization of:

$$\Delta^{30}Si_{silicate-metal} = \frac{7.6\ (\pm 0.7)\times 10^6 (1SD)}{T^2}.$$

This fit is in good agreement with the relation determined based on other enstatite achondrites (Ziegler et al., 2010) [$7.64\ (\pm\ 0.47) \times 10^6)/T^2$] and with the experiments of Shahar et al. (2009) [$7.45\ (\pm\ 0.41) \times 10^6)/T^2$]. It is, however, of slightly larger magnitude than the relationship estimated based on the experiments of Hin et al. (2014) [4.42 ($\pm$ 0.05) $\times 10^6)/T^2$] (Figure 2).

Implications for Earth's core formation

In many previous studies, the $\Delta^{30}Si_{metal\text{-}silicate}$ parametrization has been coupled with estimates for the Si isotopic offset between bulk silicate Earth (BSE) and chondrites ($\Delta^{30}Si_{BSE\text{-}chond}$) to calculate a mass-balance estimate of the amount of Si present in Earth's core (e.g. Armytage et al., 2011; Georg et al., 2007; Savage et al., 2014; Shahar et al., 2009). Unfortunately, these models are extremely sensitive to the measured $\Delta^{30}Si_{BSE\text{-}chond}$ and can predict a wide range of values, with large uncertainties, which easily overlap with the outer core mass deficit based on other methods. Instead, here we calculate the maximum effect of core formation on the Si isotopic composition

313 of the BSE using our new parametrization, and based on that, estimate the Si isotope
314 composition of the bulk Earth.

315 Both single stage core formation and continuous core formation using the most
316 modern high-pressure high temperature metal/silicate partitioning data suggest that the
317 core must contain between 2 wt. % and 9 wt. % of Si (e.g. Fischer et al., 2015; Rubie et
318 al., 2015; Siebert et al., 2013). The permitted range for the temperature of core-mantle
319 equilibrium at the base of a magma ocean is roughly 3200-4300 K in order to explain
320 moderately siderophile abundances on the Earth's mantle (Badro et al., 2015; Siebert et
321 al., 2013). Using these parameters, we have calculated the maximum isotope effect that
322 core formation can have imparted on the Si isotope composition of the BSE. Following
323 the model delineated in Savage et al. (2014), for a single-stage core formation model,
324 the effect of core formation on the Si isotopic composition is plotted in Figure 3 as a
325 function of the increase in Si in the core (from 2 to 9 wt.%) (parameters used in the
326 model are indicated in the figure caption). The two lines plotted in Figure 3 are the
327 calculated δ^{30}Si isotope composition of the bulk Earth, for two temperatures of
328 equilibration (3200 K and 4300 K). If the core contains less than 7% Si, as suggested by
329 several studies based on elemental partitioning and physical properties (Antonangeli et
330 al., 2010; Badro et al., 2015), the bulk Earth must be heavier than any chondrites.

331 As can be seen even for the most extreme calculated case (3200 K equilibration
332 temperature and 9% Si in the core) this cannot account for 0.14 ‰ of the difference
333 between the chondrites and the Earth. In other words, the Si composition of the bulk
334 Earth may be at the lightest -0.43 % (note this value is extreme as core formation is

335 unlikely to have remained at 3200mK throughout Earth's differentiation). If we use less
336 extreme parameters (e.g. T = 3800 K, Si in core = 6 wt.%) we calculate a bulk Earth
337 value of ~ -0.35 ‰. This value ~0.10 ‰ heavier than ordinary and carbonaceous
338 chondrites and ~0.20 ‰ heavier than enstatite chondrites (see Figure 4) (Armytage et
339 al., 2011; Fitoussi et al., 2009; Savage and Moynier, 2013; Zambardi et al., 2013).
340 The difference between the Si isotopic composition of the bulk silicate Earth and
341 chondrites may be due to either 1) inaccuracies in the estimation of the Si isotopic
342 composition of the BSE or 2) that the bulk Earth has a non-chondritic Si isotopic
343 composition.
344 ***Do we have an accurate estimate of the Si isotope composition of Earth's mantle?***
345 Silicon isotopes are very weakly fractionated by partial melting and fractional
346 crystallization. For example Savage et al. (2010) showed that ultramafic various mantle
347 rocks, MORBs and Island Arc basalts have all similar isotopic composition within error
348 and estimated the BSE to be at -0.29 ± 0.08 ‰. These findings are very consistent with
349 most other studies (e.g. Armytage et al., 2011; Fitoussi et al., 2009; Zambardi et al.,
350 2013; Ziegler et al. 2010) and combining all these data together Savage et al. (2014)
351 recommend a δ^{30}Si=-0.29 ± 0.07 ‰ for the composition of the BSE, which seems to be
352 a robust estimate of the Earth's upper mantle composition. More recently, it has been
353 shown that high degree partial melting from the Archean mantle, komatiites, have
354 identical composition (-0.29 ± 0.02 ‰, Deng et al., 2019), giving further support to
355 previous estimates of the BSE.

356 It should be kept in mind, however, that all the above BSE estimates are based on
357 samples derived from the upper mantle, and it has been posited that the lower mantle
358 may have a different isotopic composition. For example, it was proposed by Huang et al.
359 (2014), based on theoretical calculations, that lower mantle high pressure phases
360 (bridgmanite) should be isotopically lighter than upper mantle phases (olivines,
361 pyroxenes). Based on these calculations, Huang et al. (2014) suggested that the lower
362 mantle could be 0.1 permil lighter than the upper mantle. Considering the proportion of
363 lower (~75%) and upper (~25%) mantle, Huang et al. (2014) calculated that it could
364 be possible for the BSE to have a δ^{30}Si of ~-0.37. It is however uncertain whether such
365 isotopic heterogeneity could fully be preserved in the lower mantle on the scale of 4.6
366 Ga or homogenized by global scale convection and still be present today (e.g.
367 Brandenburg et al., 2008; Stixrude and Lithgow-Bertelloni, 2012). In further evidence
368 against an isotopically layered mantle, Pringle et al. (2016) reported a large set of data
369 for Ocean Island basalts from various localities, which were mostly undistinguishable
370 (-0.32 +/- 0.09) from the isotopic composition reported by Savage et al. (2010). While
371 some samples measured by Pringle et al. (2016) were found to have δ^{30}Si values 0.1 ‰
372 lower than upper mantle samples, these were not common, and although this paper
373 argued for the existence of some mantle heterogeneity (introduced by recycling of
374 crust), given the paucity of these isotopically “light” samples, it is unlikely that the bulk
375 of the lower mantle will be drastically different from the upper mantle, at least not to the
376 level of difference needed to bring the BSE to chondritic values (Pringle et al., 2016).

We therefore suggest that the value of -0.29 ± 0.08 ‰ for the Earth's mantle is accurate and representative of the BSE, and therefore explore the possibility that the bulk Earth is non-chondritic in terms of its Si isotope composition.

The Bulk Earth has a non-chondritic Si isotope composition

We here consider that the bulk Earth has a heavier Si isotope composition than all known chondrites groups. First, there is always the possibility that none of the chondrites from our collection represent the Si isotope composition of the Earth's precursors materials – and that all of the Earth-chondrites accreted to the Earth (Drake and Righter, 2002), and/or that Earth is an end-member Si isotopic composition, similar to the arguments made for r-process anomalies (Fischer-Godde and Kleine, 2017). However, given the small degree of variation in the Si isotope composition of all chondrite groups, it more likely that Si that accreted to form the Earth started in the solar nebula with a "chondritic" composition, and was subsequently fractionated prior to or during accretion. Pringle et al. (2014) found that angrite meteorites, that are most likely sampling a small parent body than Earth, are isotopically heavier than chondrites by ~ 0.1 ‰. Since these samples are among the most volatile depleted samples in the solar system, it was suggested that the parent body of the angrite meteorites experienced volatile loss that resulted in a preferential loss of the lighter Si isotopes. Pringle et al. (2014) suggested that this volatile loss could also have affected Earth's precursors materials and would therefore increase the bulk Earth Si isotopic composition. It was further suggested that based on model of volatile loss from

399 planetesimals and isotopic fractionation under equilibrium that ~15% Si loss could
400 explain the composition of the Earth within the first Myrs of the Solar System (Young
401 et al., 2019). Alternatively, Dauphas et al. (2015) invoke Si isotopes fractionation
402 between condensing solids and the nebula gas, and that Earth's precursors were
403 depleted in refractory phases (forsterite), decreasing its Mg/Si ratio and increasing δ^{30}Si.
404 This alternative scenario may also explain part of the Si isotopic fractionation of the
405 bulk Earth, however, it should be noted that there is a weak (coefficient of
406 determination, $R^2 = 0.5$**)** relationship between the δ^{30}Si and the Mg/Si ratio for primitive
407 meteorites and the Earth (see Figure 4).
408 We therefore suggest that Earth's precursor material underwent volatile depletion
409 during its accretion such that its Si isotope composition was fractionated from the
410 "chondritic" baseline, to a heavier isotopic composition (Hin et al., 2017; Pringle et al.,
411 2014; Young et al., 2019) . Core formation then further drove this bulk Earth value to its
412 current composition, which we measure today.
413
414 **5. Conclusions**
415 We have used an enstatite meteorite, Itqyi, as a natural experiment to determine the
416 Si isotopic fractionation factor between metal and silicate. To reach this goal, we have
417 performed a petrological and isotopic study of the meteorite in order to determine the
418 temperature of equilibrium as well as the Si isotopic composition between the phases.
419 We find that the dependence of Si isotopes with temperature to be 1530 K ± 110 K. We
420 use this dependence together with various core formation model and composition to

421 estimate the bulk Earth δ^{30}Si. We show that the bulk Earth must be isotopically heavier
422 than any chondrites groups, save that the lower mantle would be isotopically light due
423 to the preservation of bridgmanite/melt isotopic fractionation in the magma ocean. In
424 agreement with previous study we suggest that volatility have shaped the composition
425 of the Earth's precursors and modified the final composition of the bulk Earth
426 compared to its original building blocks.
427
428 **Acknowledgments:** We deeply thank the two reviewers for insightful comments and
429 for correcting important mistakes and Raj Dasgupta for efficient editing. This paper has
430 been written during a visit of FM to CUG Wuhan in October 2019. FM thanks
431 Yongsheng Liu and Jiubin Chen for making this visit possible. F. M. acknowledges
432 funding from the European Research Council under the H2020 framework
433 program/ERC grant agreement (#637503-Pristine).
434

References

Abraham, K., Opfergelt, S., Fripiat, F., Cavagna, A., deJong, J.T.M., Foley, S.F., André, L., Cardinal, D., 2008. δ^{30}Si and δ^{29}Si determinations on USGS BHVO-1and BHVO-2 reference materials with a newc onfiguration on a Nu plasma multi-collector ICP-MS. Geostand. Geoanal. Res 32, 193-202.

Antonangeli, D., Siebert, J., Badro, J., Farber, D., Fiquet, G., Morard, G., Ryerson, .F., 2010. Composition of the Earth's inner core from high-pressure sound velocity measurements in Fe-Ni-Si alloys. Earth Planet. Sci. Lett. 295, 292-296.

Armytage, R.M.G., Georg, R., Savage, P., Williams, H., Halliday, A., 2011. Silicon isotopes in meteorites and planetary core formation. Geochim. Cosmochim. Acta 75, 3662-3676.

Badro, J., Brodholt, J., Piet, H., Siebert, J., Ryerson, F.J., 2015. Core formation and core composition from coupled geochemical and geophysical constraints. Proc. Natl. Acad Sci U S A 112, 12310-12314.

Berthet, S., Malavergne, V., Righter, K., 2009. Melting of the Indarch meteorite (EH4 chondrite) at 1 GPa and variable oxygen fugacity: Implications for early planetary differentiation processes. Geochim Cosmochim Acta 73, 6402-6420.

Birch, F., 1964. Density and composition of mantle and core. J.Geophys.Res. 69, 4377–4388.

Bonnand, P., Halliday, A., 2018. Oxidized conditions in iron meteorite parent bodies. Nature Geoscience 11, 401-404.

Brandenburg, J., Hauri, E., van Keken, P., Ballentine, C., 2008. A multiple system study of the geochemical evolution of the mantle with force-balanced plates and thermochemical effects. Earth Planet. Sci. Lett. 276, 1-13.

Corgne, A., Keshav, S., Wood, B.J., McDonough, W.F., Fei, Y., 2008. Metal–silicate partitioning and constraints on core composition and oxygen fugacity during Earth accretion. Geochim. Cosmochim. Acta 72, 574.

Creech, J., Baker, J., Handler, M., Lorand, J., Storey, M., Moynier, F., Bizzarro, M., 2017. Late accretion history of terrestrial planets inferred from stable isotopes. Geochemical Perspective Letters 2, 94-104.

Dauphas, N., Poitrasson, F., Burkhardt, C., Kobayashi, H., Kurozawa, K., 2015. Planetary and meteoritic Mg/Si and δ^{30}Si variations inherited from solar nebula chemistry. Earth Planet. Sci. Lett. 427, 236-248.

Deng, Z., Chaussidon, M., Guitreau, M., Puchtel, I., Dauphas, N., Moynier, F., 2019. An oceanic subduction origin for Archaean granitoids revealed by silicon isotopes. Nature Geoscience 12, 774-778.

Drake, M.J., Righter, K., 2002. Determining the composition of the Earth. Nature 416, 39-44.

Fischer, R., Nakajima, Y., Campbell, A.J., Frost, D.J., Harries, D., Langenhorst, F., Muajima, N., Polock, K., Rubie, D.C., 2015. High pressure metal–silicate partitioning of Ni, Co, V, Cr, Si, and O. Geochim. Cosmochim. Acta 167, 177-194.

Fischer-Godde, M., Kleine, T., 2017. Ruthenium isotopic evidence for an inner Solar System origin of the late veneer. Nature 541, 525-527.

Fitoussi, C., Bourdon, B., 2012. Silicon Isotope Evidence Against an Enstatite Chondrite Earth. Science 335, 1477–1480.

Fitoussi, C., Bourdon, B., Kleine, T., Oberli, F., Reynolds, B.C., 2009. Si isotope systematics of meteorites and terrestrial peridotites: implications for Mg/Si fractionation in the solar nebula and for Si in the Earth's core. Earth Planet. Sci. Lett. 287, 77-85.

Fujii, T., Pringle, E., Chaussidon, M., Moynier, F., 2015. Isotope fractionation of Si in protonation/deprotonation reaction of silicic acid: A new pH proxy. Geochim. Cosmochim. Acta 168, 193-205.

Georg, B., Reynolds, B.C., Frank, M., Halliday, A., 2006. New sample preparation techniques for the determination of Si isotopic compositions using MC-ICPMS. Chem. Geol. 235, 95–104.

Georg, R.B., Halliday, A.N., Schauble, E.A., Reynolds, B.C., 2007. Silicon in the Earth's core. Nature 447, 1102-1106.

Hin, R., Burkhardt, C., Schmidt, M., Bourdon, B., Kleine, T., 2013. Experimental evidence for Mo isotope fractionation between metal and silicate liquids. Earth Planet. Sci. Lett. 379, 38-48.

Hin, R., Fitoussi, C., Schmidt, M., Bourdon, B., 2014. Experimental determination of the Si isotope fractionation factor between liquid metal and liquid silicate. Earth Planet. Sci. Lett. 387, 55-66.

Hin, R.C., Coath, C.D., Carter, P.J., Nimmo, F., Lai, Y.J., Pogge von Strandmann, P.A.E., Willbold, M., Leinhardt, Z.M., Walter, M.J., Elliott, T., 2017. Magnesium

isotope evidence that accretional vapour loss shapes planetary compositions. Nature 549, 511-515.

Hopp, T., Fischer-Godde, M., Kleine, T., 2018. Ruthenium isotope fractionation in protoplanetary cores. Geochim. Cosmochim. Acta 223, 75-89.

Huang, F., Wu, Z., Huang, S., Wu, F.Y., 2014. First-principles calculations of equilibrium silicon isotope fractionation among mantle minerals. Geochim. Cosmochim. Acta 140, 509–520.

Mahan, B., Siebert, J., Blanchard, I., Badro, J., Kubik, E., Sossi, P., Moynier, F., 2018. Investigating Earth's Formation History Through Copper and Sulfur Metal- Silicate Partitioning During Core- Mantle Differentiation. J. Geophys. Res.123, 8349-8363

Patzer, A., Hill, D.H., Boynton, W.V., 2001. Itqiy: A metal-rich enstatite meteorite with achondritic texture. Meteorit. Planet. Sci. 36, 1495-1505.

Patzer, A., Hill, D.H., Boynton, W.V., Frank, L., Schultz, L., Hull, T., McHargue, L., Franchi, I.A., 2002. Itqiy: A study of noble gases and oxygen isotopes including its terrestrial age and a comparison with Zaklodzie. Meteorit. Planet. Sci. 37, 823-833.

Poitrasson, F. 2017, Silicon isotope geochemistry. In review in mineralogy and geochemistry vol. 82, Non traditional stable isotopes. Editors: Teng, Dauphas, Watkins, publisher MSA, pp.289-344

Pringle, E., Moynier, F., Savage, P., JAckson, M., Moreira, M., Day, J., 2016. Silicon isotopes reveal recycled altered oceanic crust in the mantle sources of Ocean Island Basalts. Geochim. Cosmochim. Acta 189, 282-295.

Pringle, E., Savage, P., Badro, J., Barrat, J.A., Moynier, F., 2013. Redox state during core formation on asteroid 4-Vesta. Earth Planet. Sci. Lett. 373, 75–82.

Pringle, E.A., Moynier, F., Savage, P.S., Badro, J., Barrat, J.A., 2014. Silicon isotopes in angrites and volatile loss in planetesimals. Proc Natl Acad Sci U S A 111, 17029-17032.

Righter, K., Drake, M.J., 2003. Partition Coefficients at High Pressure and Temperature, Treatise on Geochemistry, Volume 2. Editor: Richard W. Carlson. Executive Editors: Heinrich D. Holland and Karl K. Turekian. pp. 568. ISBN 0-08-043751-6. Elsevier, 2003., p.425-449, pp. 425-449.

Roskosz, M., Luais, B., Watson, H.C., Toplis, M.J., Alexander, C.M.O.D., Mysen, B.O., 2006. Experimental quantification of the fractionation of Fe isotopes during metal segregation from a silicate melt. Earth Planet. Sci. Lett. 248, 851-867.

Rubie, D.C., Jacobson, S.A., Morbidelli, A., O'Brien, D.P., Young, E.D., de Vries, J., Nimmo, F., Palme, H., Frost, D.J., 2015. Accretion and differentiation of the terrestrial planets with implications for the compositions of early-formed Solar System bodies and accretion of water. Icarus 248, 89-108.

Savage, P., Armytage, R., Georg, B., Halliday, A., 2014. High temperature silicon isotope geochemistry. Lithos 190, 500-519.

Savage, P., Georg, B., Armytage, R., Williams, H., Halliday, A., 2010. Silicon isotope homogeneity in the mantle. Earth Planet. Sci. Lett. 15, 139-146.

Savage, P., Moynier, F., 2013. Silicon isotopic variation in enstatite meteorites: Clues to their origin and Earth-forming material. Earth Planet. Sci. Lett. 361, 487-496.

Savage, P., Moynier, F., Chen, H., Shofner, G., Siebert, J., Badro, J., Puchtel, I.S., 2015. Copper isotope evidence for large-scale sulphide fractionation during Earth's differentiation. Geochemical Perspective Letters 1, 53-64.

Shahar, A., Elardo, S., Macris, C., 2017. Equilibrium fractionation of non-traditional stable isotopes: an experimental perspective, In review in mineralogy and geochemistry vol. 82, Non traditional stable isotopes. Editors: Teng, Dauphas, Watkins, publisher MSA, pp. 65-83.

Shahar, A., Ziegler, K., Young, E.D., Ricolleau, A., SChauble, E.A., Fei, Y.W., 2009. Experimentally determined Si isotope fractionation between silicate and Fe metal and implications for Earth's core formation. Earth Planet. Sci. Lett. 288, 228-234.

Siebert, J., Badro, J., Antonangeli, D., Ryerson, R., 2013. Terrestrial accretion under oxidizing conditions. Science 338, 1194-1197.

Siebert, J., Corgne, A., Ryerson, F.J., 2011. Systematics of metal–silicate partitioning for many siderophile elements applied to Earth's core formation. Geochim. Cosmochim. Acta 75, 1451-1489.

Sikdar, J., Rai, V., 2020. Si-Mg isotopes in enstatite chondrites and accretion of reduced planetary bodies. Scientific Reports, 1273.

Stixrude, L., Lithgow-Bertelloni, C., 2012. Geophysics of chemical heterogeneity in the mantle. Ann. Rev. Earth Planet. Sci. 40, 569-595.

Wade, J., Wood, B.J., 2005. Core formation and the oxidation state of the Earth. Earth Planet. Sci. Lett. 236, 78-95.

Young, E.D., Shahar, A., Schlichting, H., Schauble, E., Tang, H., Labidi, J., 2019. Near-equilibrium isotope fractionation during planetesimal evaporation. Icarus 323, 1-15.

Zambardi, T., Poitrasson, F., Corgne, A., Meheut, M., Quitté, G., Anand, M., 2013. Silicon isotope variations in the inner solar system: Implications for planetary formation, differentiation and composition. Geochim Cosmochim Acta 121, 67-83.

Ziegler, K., Young, E.D., Schauble, E.A., Wasson, J.T., 2010. Metal–silicate silicon isotope fractionation in enstatite meteorites and constraints on Earth's core formation. Earth Planet. Sci. Lett. 295, 487-496.

Figure Captions:

Figure 1: Backscattered image of the Itqyi sample utilized in this study. The white phases represents the Fe-rich metal while the dark phases represents the enstatite minerals.

Figure 2: $\Delta^{30}Si_{silicate\text{-}metal}$ as a function of temperature. The $\Delta^{30}Si_{silicate\text{-}metal}$ obtained for Itqyi is reported. The two curves represent the estimated relation of $\Delta^{30}Si_{silicate\text{-}metal}$ vs temperature from Shahar et al. (2009) and Hin et al. (2014).

Figure 3: Modeled silicon isotopic composition of the bulk Earth as a function of Si content of the core for two temperatures of equilibrium (3200K and 4300K) using the isotopic fractionation factor determined in this study. For the parameters used in the model we used: Mass fraction of the BSE=0.67, mass fraction of the core = 0.33, mass fraction of Si in the BSE = 0.212, δ^{30}Si(BSE)=-0.29±0.08 (Savage et al. 2014), $\Delta^{30}Si_{silicate-metal} = \frac{7.6\ (\pm 0.7)\times 10^6}{T^2}$.

Figure 4: δ^{30}Si as a function of Mg/Si ratio for various chondrites and the Earth (using the updated δ^{30}Si for the bulk Earth calculated in the present study). The Si isotopic composition of the meteorites are from literature (Armytage et al., 2011; Fitoussi and Bourdon, 2012; Fitoussi et al., 2009; Zambardi et al., 2013).

Table Captions:

Table 1: Electron probe microanalyses of enstatite and metal phases.

Table 2: Silicon isotopic composition of the different samples analyzed in this study.

645 **Table 1.** Electron probe microanalyses of enstatite and metal phases.

646

647

Wt%	Itqiy (Enstatite)	Wt%	Itqiy (Metal)
MgO	37.050 (1.098)	**Fe**	88.960 (0.660)
SiO_2	59.404 (0.383)	**Si**	2.436 (0.129)
Al_2O_3	0.560 (0.022)	**Ni**	4.441 (0.175)
FeO	0.061 (0.018)	**Cr**	0.210 (0.015)
CaO	1.616 (0.052)	**Co**	0.284 (0.012)
TiO_2	0.029 (0.017)	**Mg**	0.136 (0.011)
Cr_2O_3	0.032 (0.010)		
Total	98.752 (0.731)	**Total**	96.467 (1.770)

Table 2. Silicon isotopic composition of the different samples analyzed in this study.

Samples	$\delta^{29}Si$	2SD	2SE	$\delta^{30}Si$	2SD	2SE	N	Description
NBS28	0.00	0.08	0.01	0.00	0.10	0.01	154	26.3 mg
NBS28-test 1	0.01	0.05	0.03	0.02	0.06	0.03	4	0.6 mg, NO_3^- match
NBS28-test 2	0.04	0.07	0.03	0.03	0.06	0.03	4	2.0 mg, NO_3^- match
BHVO-2	-0.14	0.06	0.01	-0.26	0.14	0.02	35	16.0 mg, NO_3^- match
BHVO-2	-0.13	0.11	0.05	-0.25	0.11	0.05	4	NO_3^- match: 0.44 N versus 0.44 N NO_3^-
Enstatite_01	-0.30	0.06	0.03	-0.64	0.16	0.08	4	NO_3^- match
Enstatite_02	-0.32	0.05	0.03	-0.69	0.09	0.05	4	NO_3^- match
Enstatite_03	-0.27	0.07	0.04	-0.52	0.07	0.04	4	NO_3^- match
Enstatite_04	-0.27	0.04	0.02	-0.50	0.07	0.04	4	NO_3^- match
Enstatite_05	-0.25	0.04	0.02	-0.49	0.07	0.04	4	NO_3^- match
Enstatite_06	-0.26	0.03	0.02	-0.58	0.03	0.01	4	NO_3^- match
Enstatite_07	-0.27	0.09	0.05	-0.56	0.08	0.04	4	NO_3^- match
Enstatite_08	-0.28	0.04	0.02	-0.56	0.16	0.08	4	NO_3^- match
Metal_01	-1.71	0.06	0.03	-3.56	0.02	0.01	4	NO_3^- match
Metal_02	-1.61	0.15	0.07	-3.16	0.30	0.15	4	NO_3^- match
Metal_03	-1.71	0.04	0.02	-3.35	0.10	0.05	4	NO_3^- match
Metal_04	-1.93	0.06	0.03	-3.74	0.04	0.02	4	NO_3^- match
Metal_05	-1.76	0.07	0.04	-3.41	0.05	0.03	4	NO_3^- match
Average Enstatite	**-0.28**	**0.04**	**0.02**	**-0.57**	**0.14**	**0.05**	**8**	
Average Metal	**-1.74**	**0.23**	**0.10**	**-3.44**	**0.44**	**0.19**	**5**	

Figure 1

Click here to download Figure: Figure 1.pdf

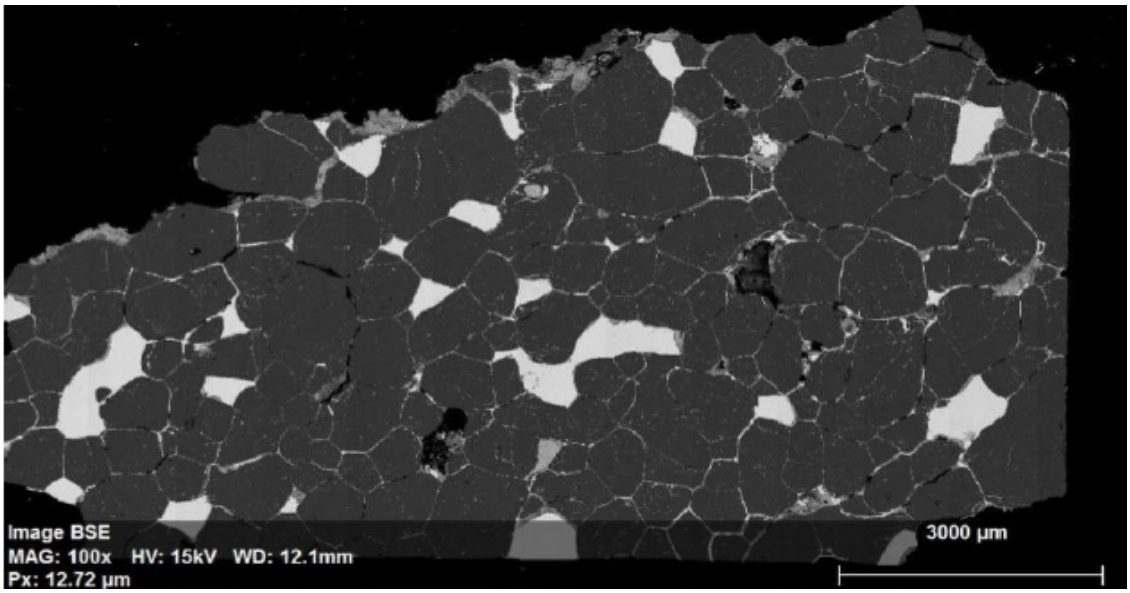

Figure 2

Click here to download Figure: Figure2.pdf

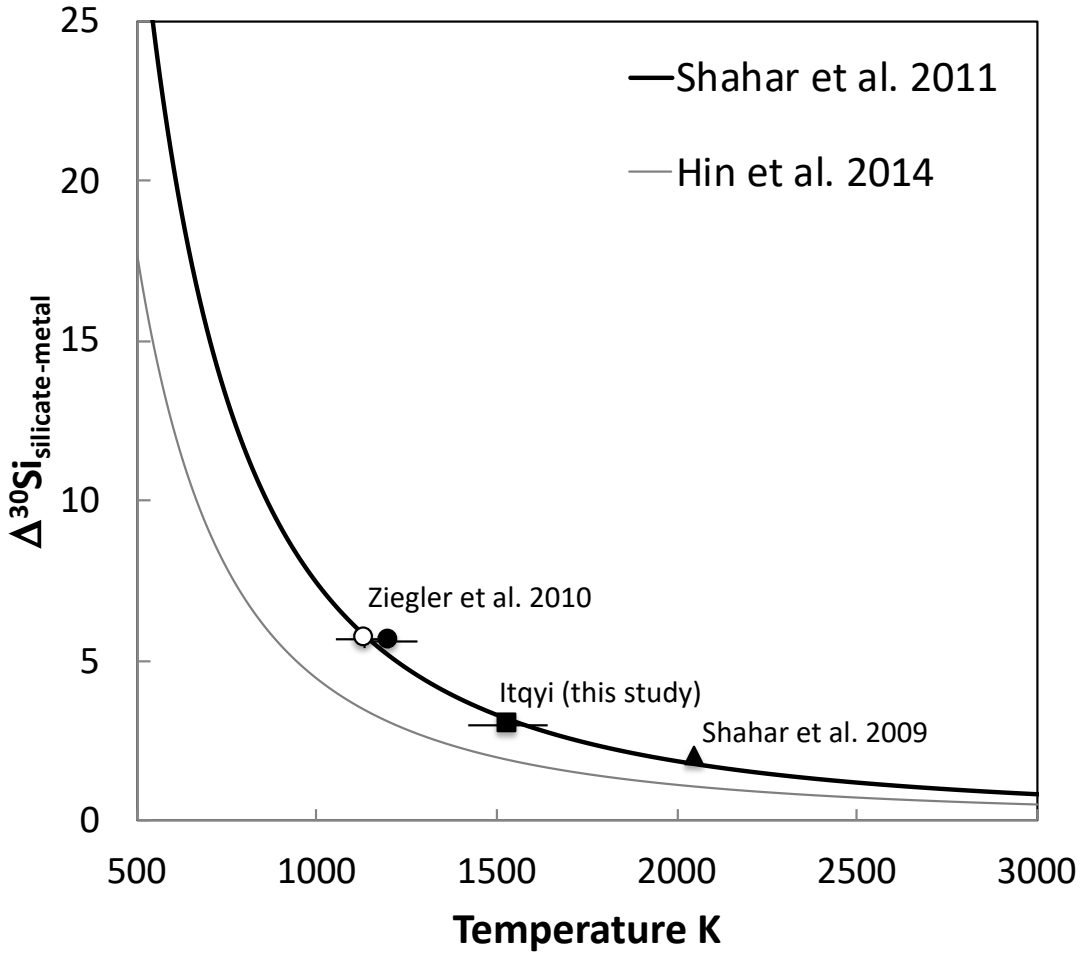

Figure 3

Click here to download Figure: Si isotope model new.pdf

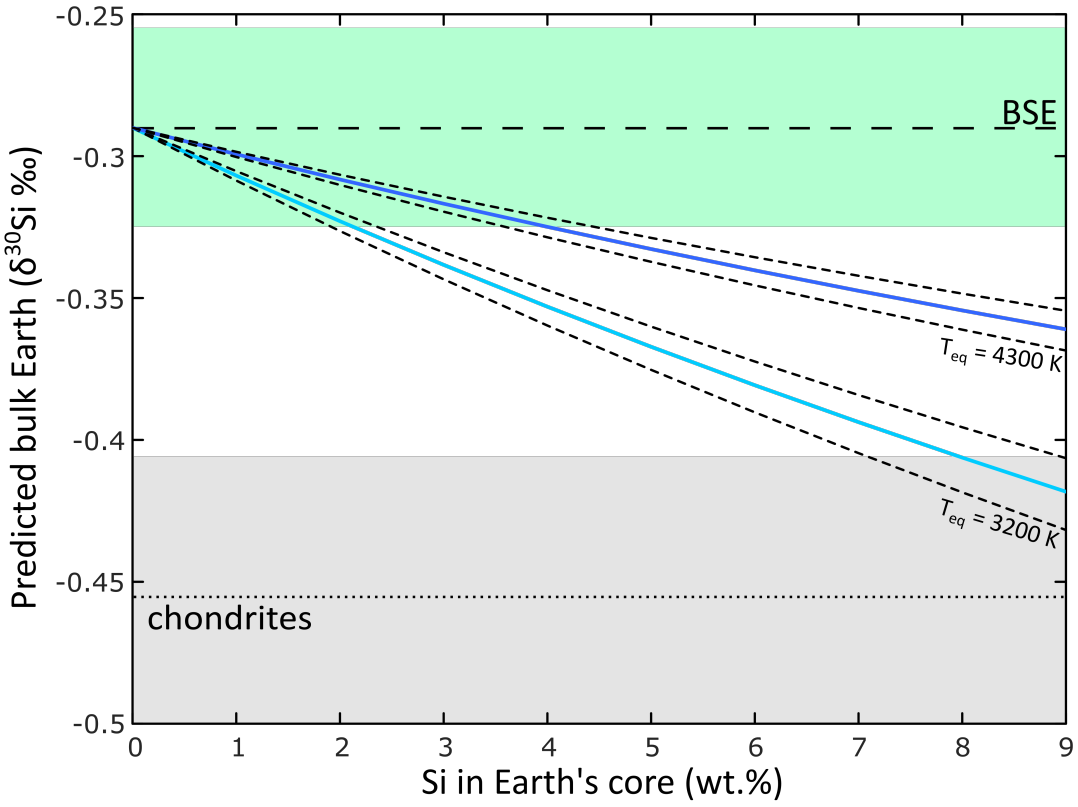

Figure 4

Click here to download Figure: Fiogure4.pdf

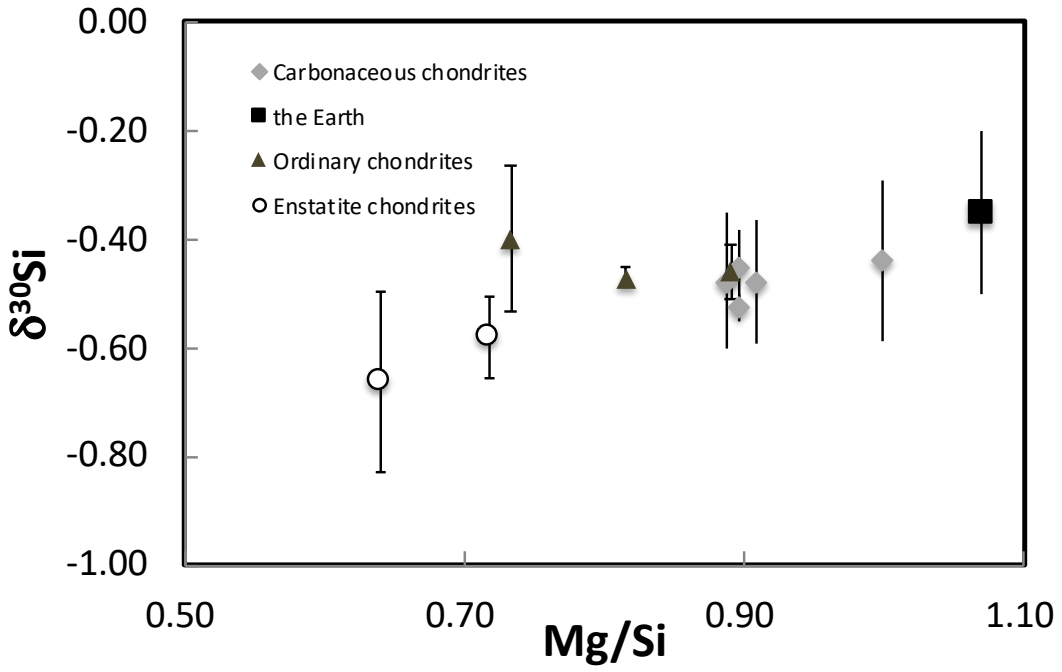

Supplementary material for online publication only

Click here to download Supplementary material for online publication only: Supplementary Materials.docx

***Declaration of Interest Statement**

Declaration of interests

☒ The authors declare that they have no known competing financial interests or personal relationships that could have appeared to influence the work reported in this paper.

☐The authors declare the following financial interests/personal relationships which may be considered as potential competing interests:

***Credit Author Statement**

Frederic Moynier: Conceptualization, interpretation, writing. Zhengbin Deng: methodology, interpretation, writing. Ariane Lanteri: methodology. Rayssa Martins: methodology. Marc Chaussidon: interpretation, writing. Paul Savage: interpretation, writing. Julien Savage: interpretation, writing.